Available online at www.sciencedirect.com
SCIENCE DIRECT®
Journal of Power Sources 118 (2003) 118–128
JOURNAL OF POWER SOURCES
www.elsevier.com/locate/jpowsour

Design considerations for effective control of an afterburner sub-system in a combined heat and power (CHP) fuel cell system (FCS)

Whitney G. Colella*

Department of Mechanical Engineering, Stanford University, Stanford, CA 94305, USA

Abstract

This article investigates various control strategies for a combined heat and power (CHP) fuel cell system (FCS), with a specific focus on the afterburner sub-system. The afterburner sub-system recovers heat and by-products from the excess fuel and oxidant not consumed within the fuel cell. The overall performance of a CHP FCS depends crucially on the control of the afterburner sub-system because the control of this sub-system (1) determines the extent of thermal energy recovered from the system, between 35 and 55% of fuel energy input; (2) establishes the rate limiting step in the control of the overall CHP FCS because the rate at which the afterburner can combust excess fuel and oxidant safely and raise steam affects the rate at which the fuel cell's electrical power output can change; and (3) impacts upstream mass and energy flows strongly, such as the system's overall water balance and also the raising of steam for the upstream fuel processor and cathode humidification, as this is the point in the system where the CHP FCS becomes closed loop for heat and mass flows. Using an Aspen Plus® chemical engineering model of the CHP FCS, this article (1) identifies potential challenges in operating the afterburner sub-system, (2) discusses various options for ameliorating those challenges, and (3) recommends viable solutions. The two challenges it discusses in detail are (1) the danger of overheating the afterburner, and (2) the danger of overheating a downstream steam generator. Regarding the first challenge, in the low anode hydrogen utilization (AHU) range (66–85%) specified by some fuel cell manufacturers, the afterburner is in danger of overheating beyond its maximum rated operating point. Regarding the second challenge, also at low anode hydrogen utilizations, the steam generator is in danger of overheating beyond its maximum rated operating point. This article demonstrates that one solution for overcoming these challenges is to dilute the afterburner's stream with exhaust gas from the cathode. This article shows the ratio of cathode exhaust flow rates that achieve the desired operating temperature regions for the afterburner and downstream sub-system components. Using this method, this article determines an optimal control strategy solution for the afterburner sub-system.

Keywords: Fuel cell system (FCS); Combined heat and power (CHP); Afterburner sub-system; Control strategy; Aspen Plus® chemical engineering model; Proton exchange membrane (PEM)

1. Introduction

Fuel cells do not consume all of their fuel; they may expel over half of their fuel without use. For a combined heat and power (CHP) fuel cell system (FCS) to achieve a high overall (combined thermal and electrical) efficiency [1], this excess fuel must be reused usefully within the system. One method for accomplishing this goal is to burn the excess fuel and oxidant in the fuel cell's exhaust gases in an afterburner, so as to recapture the chemical energy of the fuel as heat for use in other parts of the system. If properly controlled, an afterburner sub-system within a CHP FCS may recapture between 35 and 55% of the lower heating value (LHV) energy of the input fuel. One such afterburner sub-system design is shown in Fig. 1 and is modeled in detail using Aspen Plus® chemical engineering software. Based on this model, this analysis develops an effective control strategy for an afterburner sub-system [2].

The article investigates various design options for a CHP FCSs afterburner sub-system. The afterburner sub-system is one sub-system within a CHP FCS that uses proton exchange membrane (PEM) fuel cells, consumes natural gas as fuel, and provides heat and electricity to a building [3]. The CHP FCS uses a fuel reforming process to convert natural gas into a hydrogen-rich gas (reformate), which is then partially consumed within the fuel cell stack to produce electricity and heat, with any remaining reformate and oxidant processed in the afterburner sub-system to capture waste heat and by-products. Fig. 1 shows this afterburner sub-system. The afterburner (labeled 1st Afterburner) combusts excess fuel from the fuel cell's anode exhaust (anode off-gas, labeled R1) with excess oxidant from the fuel cell's cathode

* Tel.: +1-650-283-2701.
E-mail address: wcolella@alumni.princeton.edu (W.G. Colella).

0378-7753/03/$ – see front matter © 2003 Published by Elsevier Science B.V.
doi:10.1016/S0378-7753(03)00069-7

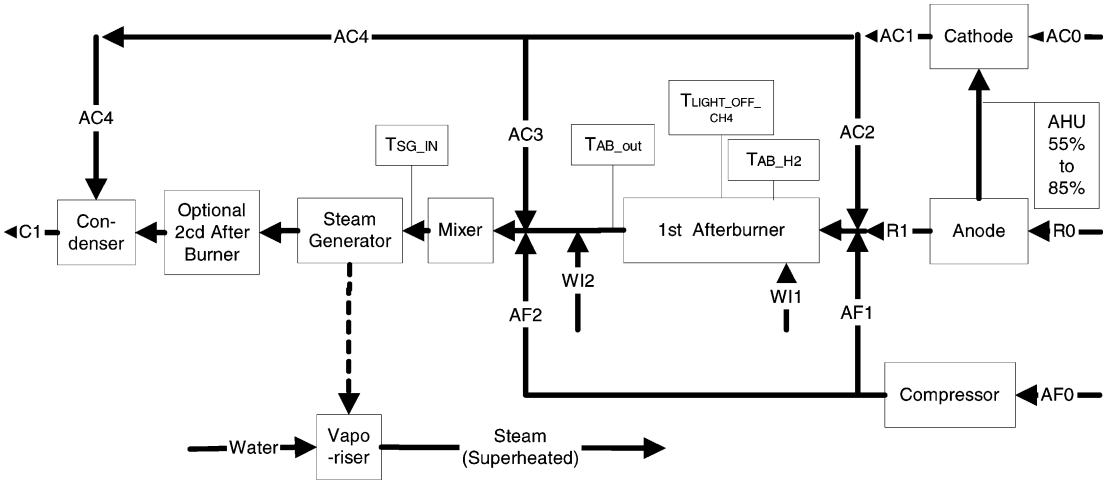

Fig. 1. Shows the afterburner sub-system of a combined heat and power (CHP) fuel cell system (FCS).

exhaust (cathode off-gas, labeled AC1) [4]. In turn, the hot afterburner exhaust is used downstream to vaporize water in a steam generator (shown in Fig. 1) for use in upstream applications. This vaporized water is used upstream (1) in the fuel cell, to humidify the cathode inlet gas; (2) in the fuel processor, to react with natural gas in the steam reforming reaction; and (3) in the fuel processor, to react with carbon monoxide in the water gas shift reaction. After vaporizing this water, the afterburner exhaust gas then passes through a condenser (shown in Fig. 1). The condenser cools this exhaust gas both (1) to capture part of the exhaust stream's heat for use in other parts of the system, and (2) to liquefy the exhaust stream's product water so that it can be recycled within the system to achieve a neutral system water balance.

This analysis (1) identifies potential problems in operating the afterburner subsection, (2) discusses various options for ameliorating those problems, and (3) recommends viable solutions. The two problems it discusses in detail are (1) the danger of overheating the afterburner, and (2) the danger of overheating the steam generator.

1.1. Problem 1

For the low anode hydrogen utilization (AHU) range (66–85%) specified by some fuel cell manufacturers for their fuel cell stack design, most stainless steel afterburners are in danger of overheating beyond their maximum rated operating point (650 °C for many).

1.1.1. Solution to Problem 1

To prevent the afterburner from over-heating, one option is to dilute the afterburner stream, for example, with (a) cathode off-gas, (b) air, or (c) water. Of these, unless the water used to cool the afterburner is later entirely condensed downstream to capture its latent heat of vaporization, dilution with cathode off-gas is the most energy efficient. This analysis concludes that, for a hydrogen utilization range that reaches as low as 55%, the amount of cathode off-gas available is large enough to dilute the afterburner stream to acceptable operating temperatures. Given a specified utilization level, the analysis determines appropriate cathode off-gas flow rates to achieve an acceptable operating temperature.

1.2. Problem 2

Also at low AHUs, system components downstream of the afterburner may be in danger of overheating. In the scenario of Fig. 1, the steam generator, positioned downstream of the afterburner and acting as its thermal sink, is in danger of overheating beyond the maximum rated operating point of most steam generators (400 °C for many).

1.2.1. Solution to Problem 2

To avoid this danger at low AHUs, one effective solution is as follows: (a) all of the cathode off-gas not fed to the afterburner can be fed to the inlet of the steam generator for cooling, no cathode off-gas is fed directly to the condenser; and (b) the steam generator can be operated above its rated operating point up to 550 °C in exchange for a shorter operating life.

2. Experimental: modeling methodology and datum design conditions

2.1. Modeling methodology

The analysis of the CHP FCS afterburner sub-system is based on a computer process model of a complete stationary fuel cell power plant producing a gross electrical power output of 6 kW. The model uses a combination of computer programs and languages: (1) Aspen Plus® steady-state chemical engineering process software (version 11.1), (2) Microsoft Excel™, (3) Fortran, and (4) Microsoft Visual Basic™.

2.2. Operating specifications

The afterburner sub-system is initially evaluated around certain operating specifications. These operating specifications are based on manufacturer's data for components (1) within the afterburner sub-system, and (2) within the fuel cell stack sub-system.

2.2.1. Afterburner sub-system

The afterburner sub-system's operating specifications are based on manufacturer's data for this sub-system's components. These components include: (1) the afterburner, (2) the afterburner catalyst, (3) the steam generator, and (4) the condenser. Most stainless steel afterburners have a maximum rated operating point below 650 °C, recommended by their manufactures. This analysis is based on a maximum rated afterburner operating temperature of 650 °C. At the same time, the afterburner's minimum operating temperature must be greater than the light-off temperature of methane in the anode exhaust gas over the afterburner's catalyst. This analysis assumes a minimum light-off temperature of 400 °C for the combustion of methane in low concentrations over a platinum group metals (PGM) catalyst. Downstream of the afterburner, the steam generator, also made of stainless steel, suffers durability concerns with increased temperatures. The steam generator is assumed to have a maximum manufacturer-recommended rated operating temperature of 400 °C, in line with the maximum rating for most stainless steel steam generators, although it can withstand 550 °C with the tradeoff of a shorter operating life. Downstream of the afterburner, the condenser, also made of stainless steel, is assumed to have a maximum operating temperature of 400 °C.

2.2.2. Fuel cell stack sub-system

The fuel cell stack sub-system's operating specifications are also based on manufacturer's data. The PEM fuel cell stack operates at temperatures between 60 and 70 °C, and at pressures between 1.082 and 1.358 bar. The fuel cell stack's polarization curve is based on experimental data for a PEM fuel cell stack run on natural gas reformate. The fuel cell stack consumes between 65 and 85% of the hydrogen supplied to it at the anode, an anode stoichiometry between 1.2 and 1.5, and consumes air at a stoichiometry of 2. A typical reformate gas fed to the fuel cell stack has a molar concentration of 33.5% H_2O, 33% H_2, 11% CO_2, 0.5% CH_4, 22% N_2 and a few ppm CO.

3. Results and discussion

3.1. Problem 1: Afterburner temperature exceeds maximum rating at low utilizations

Based on the Aspen Plus® chemical engineering model of the afterburner sub-system, Fig. 2 shows that the adiabatic outlet temperature of gases from the afterburner (T_{AB_OUT}) is higher than the afterburner's maximum rated operating

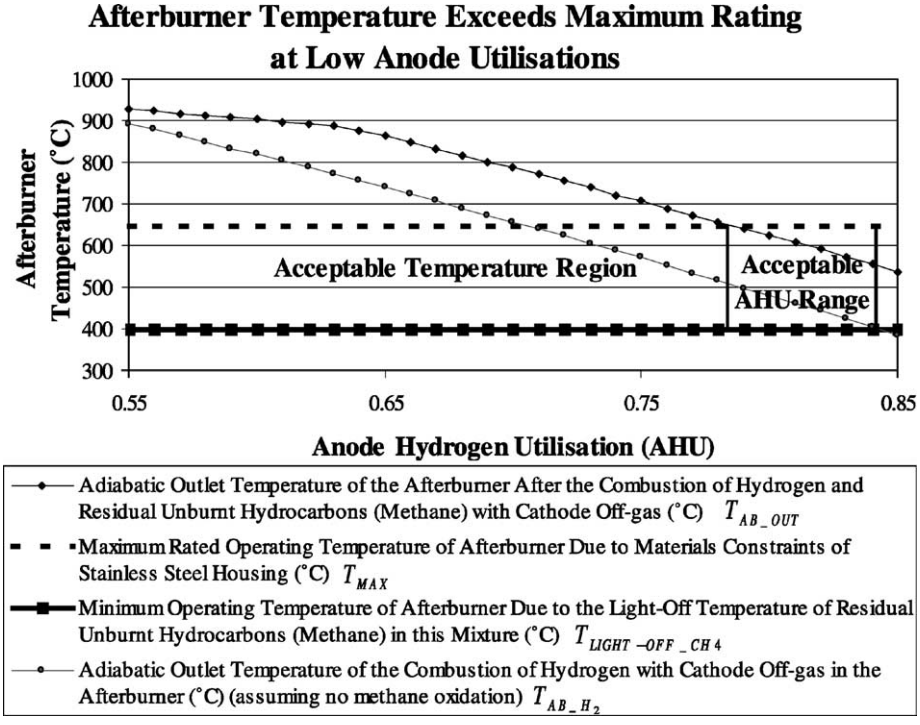

Fig. 2. The afterburner is best operated below an exit temperature of 650 °C due to materials constraints and above a hydrogen flame temperature of 400 °C due to the light-off temperature for methane under a particular catalyst.

temperature (T_{MAX}) at all utilizations below 82%. The afterburner's outlet temperature (T_{AB_OUT}) is labeled in the schematic diagram of Fig. 1. As a result of low anode hydrogen utilization, the afterburner temperature may rise above its maximum rating. The afterburner's temperature is limited on the high end due to either the reduction in lifetime of the external stainless steel casing or the sintering of the catalyst. For the specified afterburner design, the maximum temperature of the external stainless steel casing is 650 °C. For the specified PEM stack design run on reformed natural gas fuel, the stack operates at a relatively low hydrogen utilization at the anode, between 65 and 85%. Although most commercial PEM stack manufacturers (including Ballard, Inc.; Honeywell, Inc.; and International Fuel Cells, Inc.) try to operate at higher utilizations between 75 and 90%, many industrial stacks operate across a lower utilization range in practice, particularly with operating use [5]. At low utilizations, a larger percentage of hydrogen flows to the afterburner, where it combusts and thereby increases the afterburner's operating temperature. As the anode hydrogen utilization decreases, the afterburner temperature rises because:

(1) the anode off-gas is composed of a larger percentage of combustible hydrogen not consumed at the anode, and
(2) the cathode off-gas is composed of a larger percentage of oxygen not consumed at the cathode.

Excess oxygen is present in the cathode off-gas because the percentage of oxygen fed to the fuel cell's cathode is higher than the stoichiometric amount for complete reaction with hydrogen so as to enhance oxygen kinetics at the cathode. Excess oxygen is also used to compensate for the effect of aging and external contaminants on the cathode [6]. Therefore, even after all hydrogen has reacted with oxygen, excess oxygen remains for the combustion of residual unburnt hydrocarbons in the anode off-gas.

The operating temperature of the afterburner is also limited at the low end. For residual unburnt hydrocarbons (methane) to combust in this mixture, the adiabatic temperature of the afterburner's gas mixture after the combustion of hydrogen ($T_{AB\_H_2}$) must be greater than the light-off temperature of methane ($T_{LIGHT\text{-}OFF\_CH_4}$). Since hydrogen combusts preferentially over methane, this minimum temperature can be achieved with a high enough hydrogen adiabatic flame temperature. The location of the afterburner's hydrogen adiabatic flame temperature is shown in the schematic diagram of Fig. 1. Both temperatures ($T_{AB\_H_2}$ and $T_{LIGHT\text{-}OFF\_CH_4}$) are plotted in Fig. 2.

The light-off temperature of methane in the presence of the afterburner's specified platinum group metals catalyst for typical afterburner concentrations was determined to be approximately 400 °C via a combination of experimental tests and Aspen Plus® chemical engineering modeling. Experimental tests recorded the synthetic anode off-gas flow rate to the afterburner, and the afterburner's outlet temperature for 24.53 and 100% conversion of methane. The hydrogen flow rate was altered for the two trials: in the first case, the hydrogen flow rate was not high enough to produce a high enough enthalpy of combustion to heat the burner to a high enough temperature to light-off all the methane, and in the second case, it was. Fig. 3 shows the experimental test set-up, results, and final conclusion of the modeling analysis. The temperature of the final outlet gases from the afterburner was taken as the first thermocouple reading outside of the catalyst block, to allow for mixing of these gases, which have a radial temperature distribution within the block. It is assumed that, at this point, the effects of back-radiation from the catalyst block and heat loss from the burner's periphery offset each other. It is assumed that this temperature reading is more accurate than one from a thermocouple in the catalyst block, which may be touching part of the block's wall and therefore produce too high a reading. Table 1 shows an independent mass and energy balance analysis for the experimental results for the afterburner. Discrepancies in energy balance were minor (+6 °C for the outlet temperature of the afterburner at 25.43% conversion and −27 °C for 100%) and can easily be attributed to heat loss (assumed zero in this analysis). Fig. 4 shows the Aspen Plus® simulation set-up, the experimentally determined temperatures that were used as inputs for the simulation, and the model's output results for methane light-off temperature (the temperatures for stream 2).

The methodology behind the Aspen Plus® simulation is described here. Based on the hydrogen flow rate and afterburner inlet temperature, the light-off temperature range of methane was equated to the adiabatic flame temperature for the combustion of hydrogen (the temperature achievable in the reactor assuming the process is adiabatic and all of the energy released by the combustion goes to raise the temperature of the combustion products) and back-calculated according to:

$$\sum_i \left[\dot{N}_i\left(\Delta\bar{H}^\circ_{f_i} + \int_{T_s}^{T_p} \bar{c}_{p_i}\,\mathrm{d}T + \bar{H}_{\mathrm{VAP}_i}\right)\right]_{\mathrm{PROD}} = -\dot{N}_{\mathrm{FUEL}}\,\Delta\bar{H}^\circ_c + \sum_i \left[\dot{N}_i\left(\Delta\bar{H}^\circ_{f_i} + \int_{T_s}^{T_r} \bar{c}_{p_i}\,\mathrm{d}T + \bar{H}_{\mathrm{VAP}_i}\right)\right]_{\mathrm{REACT}}, \quad (1)$$

and

$$\bar{c}_{pi} = a + bT + cT^2 + dT^3, \quad (2)$$

where $\dot{N}_i$ is the molar flow rate of species i, $\Delta\bar{H}^\circ_{f_i}$ the standard molar enthalpy of formation for species i, $\bar{c}_{p_i}$ the molar heat capacity of species i at temperature T, $\bar{H}_{\mathrm{VAP}i}$ the molar enthalpy of vaporization for species i (if applicable), $\dot{N}_{\mathrm{FUEL}}$ the molar flow rate of fuel (in this case hydrogen), $\Delta\bar{H}^\circ_c$ the standard molar enthalpy of combustion for that fuel, T_p is the temperature of the products, T_r the temperature of the reactants, and T_s the temperature at which standard enthalpy of formation is tabulated (25 °C) [7]. This analysis takes the composition and temperature of the products to be after the

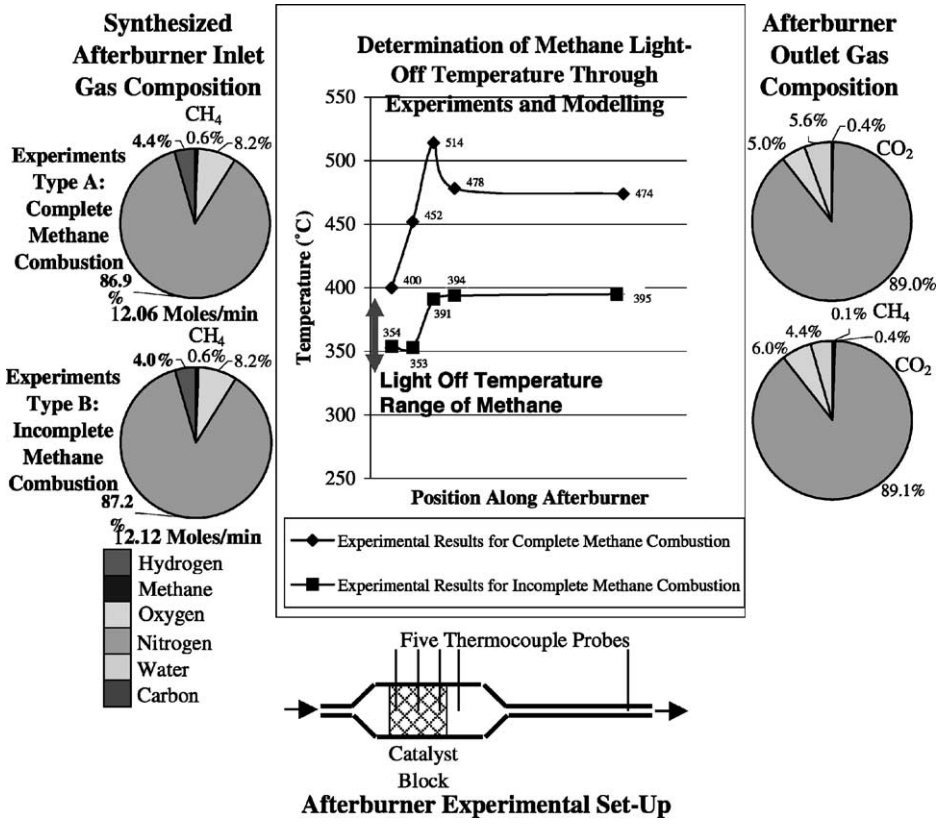

Fig. 3. Afterburner experimental set-up.

combustion of hydrogen but before the combustion of methane. The equation is solved iteratively for the temperature of the products, T_p, assuming

$$T_{\text{LIGHT-OFF\_CH}_4} = T_{\text{AB\_H}_2} = T_p. \quad (3)$$

Under these assumptions, the light-off temperature range was 352 °C for 25.43% conversion of methane and 386 °C for 100% conversion, shown in cases C and A in Fig. 4. This estimate is conservatively on the high end in that it assumes that all hydrogen combusts before methane and that no heat is lost during the combustion of hydrogen. Performing a similar calculation based on the outlet temperature of the afterburner and the enthalpy of the combusted methane, these temperatures were 357 °C for 25.43% conversion of methane and 331 °C for 100% conversion, shown in cases B and D in Fig. 4. This estimate is conservatively on the low end in that it assumes that no heat is lost during the combustion of methane. Fig. 4 summarizes the experimentally determined temperatures that were used as inputs for the model and the model's output results for methane light-off (the temperatures for stream 2). From this analysis, one can conclude that the methane light-off temperature is in the range of 330–390 °C. Although this temperature range is wide, it is precise enough for defining the parameter of minimum operating temperature for the afterburner in the large fuel cell system model.

Temperature (°C)

Case	Experimental Result Stream 1	Modelling Result Stream 2	Experimental Result Stream 3	Methane Conversion (%)
A	25	386	--	100.00%
B	–	331	478	100.00%
C	25	352	--	24.53%
D	–	357	394	24.53%

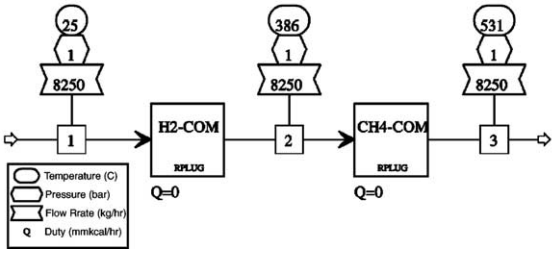

Fig. 4. Aspen Plus® model to derive light-off temperature.

Based on these estimates, and allowing for measurement error to ensure that all methane is combusted, and allowing for the effects of catalyst aging, it is prudent to define the light-off temperature constraint at 400 °C. A constraint at 400 °C creates enough of a safety factor to allow for some lag-time in dynamic changes in the system, for example, if the fuel cell's utilization increases rapidly, the hydrogen flow rate decreases to the extent that there may not be enough hydrogen to light-off the residual methane and consequently the afterburner flame extinguishes and the steam generator floods. Based on this 400 °C light-off temperature constraint, Fig. 2 shows that the hydrogen flame temperature

Table 1
Determining methane light-off temperature on platinum group metals catalyst

Component	Raw data Volumetric flow (SLM)	Calculated data			Raw data Volumetric flow (SLM)	Calculated data		
		Molar flow (mol/min)	Mole fraction	Enthalpy (kJ/m)		Molar flow (mol/min)	Mole fraction	Enthalpy (kJ/m)
	Experimental results type A: complete hydrogen combustion; complete methane combustion (inlet conditions)				Experimental results type B: Complete hydrogen combustion; incomplete methane combustion (24.53% conversion) (inlet conditions)			
CH_4	1.51E+00	6.74E−02	5.56E−03	−5.05E+00	1.51E+00	6.74E−02	5.59E−03	−5.05E+00
Air	1.06E+02	4.73E+00	3.91E−01	0	1.06E+02	4.73E+00	3.92E−01	0
N_2 as dilutant	1.52E+02	6.79E+00	5.60E−01	0	1.52E+02	6.79E+00	5.63E−01	0
H_2	1.19E+01	5.31E−01	4.38E−02	0	1.07E+01	4.78E−01	3.96E−02	0
Total	2.71E+02	1.21E+01	1	−5.05E+00	2.70E+02	1.21E+01	1.00E+00	−5.05E+00
O_2 in air		9.94E−01	8.20E−02			9.94E−01	1.87E+00	
N_2 in air		3.74E+00	3.09E−01			3.74E+00	7.04E+00	
Total N_2 (air and dilutant)		1.05E+01	8.69E−01		1.05E+01	8.72E−01		
Carbon		6.74E−02				6.74E−02		
Inlet temperature (C)	25				25			
Ambient temperature (°C)	20				20			
Inlet pressure (atm)	1.04E+00				1.04E+00			
Ambient pressure (atm)	9.87E−01				9.87E−01			
Component	Raw data Mole fraction (dry gas)	Calculated data			Raw data Mole fraction (dry gas)	Calculated data		
		Molar flow (mol/min)	Enthalpy (kJ/m)			Molar flow (mol/min)	Enthalpy (kJ/m)	
	Experimental results type A: complete hydrogen combustion; complete methane combustion (outlet conditions)				Experimental results type B: Complete hydrogen combustion; incomplete methane combustion (24.53% conversion)			
Dry total		1.12E+01				1.13E+01		
H_2	0	0	0		0	0	0	
CO_2	4.15E−03	4.64E−02	−1.73E+01		1.30E−03	0	−5.56E+00	
CH_4	0	0	0		4.00E−03	0	−2.66E+00	
N_2	Remainder	1.05E+01	1.43E+02		Remainder	1.05E+01	1.15E+02	
CO	0	0	0		0	0	0	
O_2	Remainder	5.89E−01	8.35E+00		Remainder	7.55E−01	8.12E+00	
H_2O	N/A	6.66E−01	−1.49E+02		N/A	6.13E−01	−1.18E+02	
Wet total		1.18E+01	−1.5E+01			1.19E+01	−2.99E+00	
Carbon		4.64E−02				0		
Carbon balance differential (%)		31.14%				1	−1.18E+02	
Percentage C conversion (outlet gas basis)		1				2.45E−01		
Percentage C conversion (inlet gas basis)		1				1		
Outlet temperature (°C)	478				394			
Test case	Temperature (°C)	Enthalpy (kJ/m)	Temperature differential (°C)		Temperature (°C)	Enthalpy (kJ/m)	Temperature differential (°C)	
	Experimental results type A: complete hydrogen combustion; complete methane combustion (outlet temperature required for enthalpy balance)				Experimental results type B: complete hydrogen combustion; incomplete methane combustion (24.53% conversion) (outlet temperature required for enthalpy balance)			
Original	478	−1.52E+01			394	−2.99E+00		
Test case #1	500	−6.96E+00	22		390	−4.46E+00	−4	
Test case #2	525	2.45E+00	47		389	−4.83E+00	−5	
Test case #3	505	−5.09E+00	27		388	−5.20E+00	−6	

is high enough to achieve light-off for all anode hydrogen utilizations <84%.

3.1.1. Summary of Problem 1: Dual temperature constraints on the afterburner

The afterburner must operate between maximum and minimum temperature constraints. First, the adiabatic outlet temperature of gases from the afterburner (T_{AB_OUT}) must be less than the afterburner's maximum rated operating temperature (T_{MAX}) of 650 °C due to the surrounding stainless steel casing, or

$$T_{AB\_OUT} < T_{MAX}. \quad (4)$$

Second, the adiabatic temperature of gases inside the afterburner after the combustion of hydrogen ($T_{AB\_H_2}$) must be greater than the light-off temperature of methane ($T_{LIGHT\text{-}OFF\_CH_4}$) at 400 °C due to the catalyst, or

$$T_{AB\_H_2} > T_{LIGHT\text{-}OFF\_CH_4}. \quad (5)$$

T_{AB_OUT} and $T_{AB\_H_2}$ are related by the enthalpy of combustion of methane, according to the previous formula. Fig. 2 shows the two temperature constraints $T_{AB\_H_2}$ and T_{AB_OUT} as horizontal boundaries and the acceptable operating region between them. Based on these two constraints, Fig. 2 concludes that the acceptable anode hydrogen utilization range is between only 78 and 84%.

3.1.2. Potential solutions to Problem 1

Given these minimum and maximum operating limits for the afterburner, its temperature must be carefully managed via one or more design options:

(1) Dilute the afterburner inlet gas with cathode off-gas. In Fig. 1, the percentage of cathode off-gas (stream AC1) flowing to the afterburner inlet is increased via stream AC2. On the one hand, dilution with nitrogen and uncombusted oxygen will have a cooling effect. On the other hand, if one adds oxygen into a fuel-rich mixture, a larger amount of combustion and a higher temperature will result.
(2) Dilute the afterburner inlet gas with air (stream AF1). This scenario has the same potential benefits and drawbacks as dilution with cathode off-gas, with the additional drawback of lower energy efficiency due in part to the additional compressor power needed. The dilution with air can be achieved in several different ways: (a) a separate stream with a separate compressor, (b) a combined stream with the fuel cell air feed stream using the same compressor but fed directly to the afterburner via a bypass, and (c) a combined stream with the fuel cell air feed stream using the same compressor and feed through to the fuel cell (essentially operating at a higher cathode stoichiometry). One benefit to this last approach is that the efficiency of the fuel cell stack may improve with better oxygen kinetics at the cathode. One drawback is the additional compressor power needed to feed this additional amount of air and the drying effect of convection against the cathode.
(3) Dilute the afterburner inlet gas with water (stream WI1). Dilution with water is less energy efficient than air or cathode gas dilution if the water vapor is not later condensed out downstream. The primary disadvantages of water-cooling are two fold. First, a downstream condensing heat exchanger may be less efficient than an equivalent downstream gaseous heat exchanger if liquid droplets physically block the gas flow. Second, and more importantly, a greater percentage of the heat available for transfer must be transferred at relatively low temperatures (below 100 °C at 1 atm). An outlet for this low-grade heat may be unavailable.
(4) Use two burners, one upstream of the steam generator (in Fig. 1 see 1st Afterburner) and the other downstream of the steam generator (in Fig. 1 see 2nd Afterburner). The first is run-rich so that it generates just enough heat to raise steam. The first burner is starved of cathode off-gas. The second is run after the afterburner stream has exchanged heat with the steam generator and burns the remaining hydrogen and all the methane. One constraint is that the temperature of burning the hydrogen must be high enough to light-off the methane (400 °C). Integrated into a domestic CHP system, the second burner could be used in place of a boiler. In this case, the second burner would have to be specially designed to accommodate a dilute hydrogen mixture with a large percentage of nitrogen and water. The mixture is too dilute to accommodate non-catalytic combustion, as found in conventional boilers.
(5) Use a heat exchanger to indirectly cool the stream temperature with another stream. The main drawback of this option is that the heat exchanger materials must withstand high temperatures.

The first of these options is investigated most thoroughly below, because it requires the least additional hardware, additional mass and energy flows, and hence system complexity. This analysis determines, for a range of anode hydrogen utilizations, if the quantity of cathode off-gas available is large enough for cooling. Based on this investigation, it then determines appropriate flow fractions to achieve the cooling.

3.1.3. Investigation of option 1: Dilute the afterburner gas with cathode off-gas

Fig. 5 shows that the outlet temperature of the afterburner can be reduced to acceptable levels by diluting the stream with cathode off-gas for the range of utilizations investigated (55–85%). Fig. 5 shows a two-dimensional plot of two independent and one dependent variable: anode hydrogen utilization (*X*-axis), cathode off-gas fraction sent to the afterburner (molar fraction of stream AC1 from Fig. 1 flowing to AC2) (*Y*-axis), and the adiabatic afterburner outlet temperature (*Z*-axis). Fig. 5 shows that for all anode

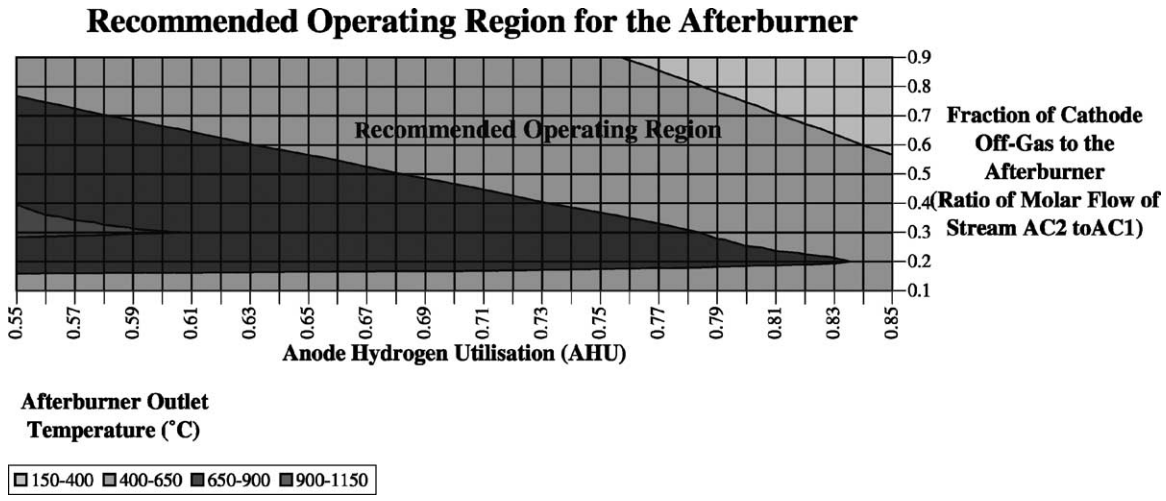

Fig. 5. Highlights the acceptable region in which to operate the afterburner in light shading. The figure indicates, for a given anode hydrogen utilization, acceptable cathode off-gas fractions at which to operate the afterburner system.

utilizations from 55 to 85%, the amount of cathode off-gas sent to the afterburner can be increased to be high enough to dilute the temperature stream to less than the burner's maximum 650 °C operating point. For all utilizations, Fig. 5 shows operating points below 650 °C and above the minimum temperature line of 400 °C depending on the fraction of cathode off-gas. For example, as shown by data in the far corner of Fig. 5, for the extreme case of a utilization of 55%, if 90% of the cathode off-gas is diverted to the afterburner, the afterburner will operate at 600 °C.

Based on this analysis, Fig. 5 summarizes the acceptable region in which to operate the afterburner in light shading. This region indicates, for a given anode hydrogen utilization, that the sub-system should be run within a band of acceptable cathode off-gas flow rates diverted to the burner. The upper limit of cathode flow rates is constrained by the need to attain a minimum operating temperature in the burner of 400 °C to combust residual unburnt hydrocarbons (methane) in the anode off-gas. The lower limit is constrained by the maximum operating temperature of the burner (650 °C) resulting from materials constraints.

The light-shaded band at the bottom of Fig. 5 refers to fuel-rich operation in which the afterburner is fed less than the stoichiometric amount of cathode off-gas. As shown by this lower band in Fig. 5, at all utilizations, the afterburner temperature can be controlled to between 650 and 400 °C by reducing the cathode off-gas fraction to 20% or less. In this scenario, the afterburner achieves low enough temperatures because not all of the anode off-gas burns. Although this operating band does achieve acceptable afterburner operating temperatures, it is an energy efficient scenario only if residual hydrogen and hydrocarbons are combusted in a second afterburner downstream of the first (see the schematic diagram of Fig. 1 for the position of the second afterburner). Therefore, for energy efficient operation with only one burner, the practical operating region is the upper light-shaded band of Fig. 5.

Although this analysis shows that it is entirely feasible to cool the afterburner with cathode off-gas, this solution deserves one important caveat. As the trend line of the dark-shaded region of Fig. 5 implies, at lower utilizations (<53%), the entirety of the cathode off-gas will not be enough to dilute the stream to acceptable operating temperatures. This is an important case to consider because anode utilization will decline as the stack ages and may exhibit low peaks during normal operation (for example, as a result of blockage of reactant pathways).

3.2. Problem 2: Steam generator temperature exceeds maximum rated temperature at low utilizations

A design challenge arises in the afterburner sub-system because the minimum outlet temperature of afterburner (400 °C) equals the maximum inlet temperature of the downstream steam generator (400 °C) if no cooling occurs in between. Fig. 1 shows the afterburner (labeled 1st Afterburner) and downstream steam generator. If the stream between these is not cooled, the adiabatic afterburner outlet temperature shown in Fig. 2 and that shown in Fig. 5 equal the inlet temperature of the steam generator as well. Even in the case in which the afterburner is cooled (for example, with cathode off-gas as shown in Fig. 5), the steam generator will overheat. As a result, the gas exiting the afterburner must be cooled before reaching the steam generator's inlet.

3.2.1. Potential solutions to Problem 2

Cooling options are similar to those discussed for Problem 1:

(1) Dilute the steam generator inlet gas with cathode off-gas (in Fig. 1 stream AC3).
(2) Dilute the steam generator inlet gas with air (stream AF2).

(3) Dilute the steam generator inlet gas with water (stream WI2).
(4) Use two burners, one upstream of the steam generator (in Fig. 1 the 1st Afterburner) and the other downstream of the steam generator (the optional 2nd Afterburner).
(5) Use a heat exchanger to indirectly cool the stream temperature with another stream.

Of these, as with Problem 1, the option requiring the least additional hardware and parasitic power is the first, which is investigated below.

3.2.2. Investigation of option 1: Dilute the steam generator inlet gas with cathode off-gas

Fig. 6 displays, for a given anode hydrogen utilization, the fraction of cathode off-gas flowing to the inlets of the afterburner and the steam generator that will achieve desired temperatures in the steam generator. This analysis is based on the simplest control method, the scenario in which all of the cathode off-gas (stream AC1 in Fig. 1) flows either to the inlet of the afterburner (AC2) or to that of the steam generator (AC3), and none directly to the condenser (AC3). In other words, the molar flow rate of stream AC3 shown in Fig. 1 ($\dot{N}_{AC3}$) is equated to the difference between that of AC1 ($\dot{N}_{AC1}$) and AC2 ($\dot{N}_{AC2}$); the molar flow rate of stream AC4 ($\dot{N}_{AC4}$) is zero:

$$\dot{N}_{AC3} = \dot{N}_{AC1} - \dot{N}_{AC2}, \quad (6)$$

$$\dot{N}_{AC4} = 0. \quad (7)$$

(Therefore, the fraction of cathode off-gas flowing to the inlet of the afterburner is unity minus the fraction shown in Fig. 6.)

Fig. 6 shows the minimum temperature that the gas stream can achieve at the inlet to the steam generator using the entirety of the cathode off-gas to cool it. For all utilizations, the cathode off-gas can dilute the inlet to the steam generator to below its maximum rated operating temperature of 400 °C. This recommended operating region is highlighted in light shading, labeled "Recommended Operating Region".

For cathode off-gas fractions between 0.4 and 0.9, the steam generator temperature converges along a line between 550 and 300 °C. This convergence results from the fact that, after all the oxygen in air has been reduced, the cathode off-gas can dilute the reformate stream either before (AC2) or after (AC3) the afterburner with the same effect on the steam generator's temperature.

Fig. 6 highlights a second region in even lighter shading, labeled "Acceptable Operating Region." Although its maximum rated temperature is 400 °C, the steam generator can be operated above this in practice up to 550 °C in exchange for a reduced operating life. The light region of Fig. 6 shows cathode off-gas flow rates that achieve temperatures within this expanded temperature range (400–550 °C). This expanded operating region needs to be called upon at lower utilizations, because the entirety of the recommended operating region does not achieve high enough temperatures to generate steam.

For part of the "Recommended Operating Region" shown in Fig. 6, the outlet temperature of the afterburner is too low to raise the required steam to 110 °C. Fig. 7 shows the recommended operating region for the steam generator given a constraint of a minimum stream exit temperature of 150 °C. The steam generator can not operate under fuel-rich conditions in the afterburner when the fraction of cathode off-gas to the steam generator is 80% or greater (shown in Fig. 7 by the bottom more darkly-shaded region). The steam generator also cannot operate under fuel lean conditions in the afterburner when the anode hydrogen utilization is 85% or greater (shown in Fig. 7 by the more darkly-shaded vertical region). The light-shaded region of Fig. 7 summarizes acceptable operating points.

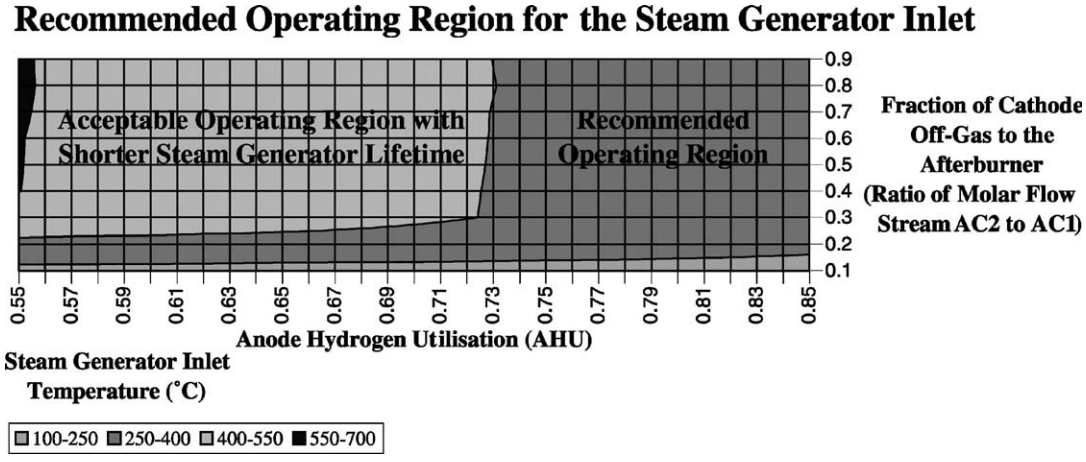

Fig. 6. Shows that even at utilizations as low as 55%, the steam generator can be cooled with the available cathode off-gas. The figure shows the effect of cathode off-gas flow rate for a given anode hydrogen utilization on steam generator operating temperature. The recommended operating temperature region for the steam generator is between 250 and 400 °C, shown by the light-shaded region. In exchange for a shorter operating life, it can be operated up to 550 °C, shown by the even more lightly-shaded region.

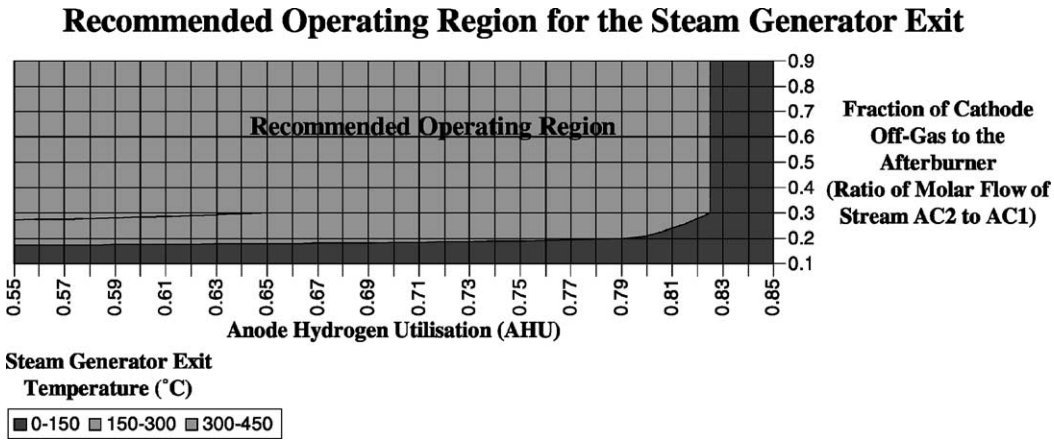

Fig. 7. Shows the recommended operating region for the steam generator given a constraint of a minimum stream exit temperature of 150 °C. The light-shaded region indicates the recommended operation region; the temperature here does not exceed 400 °C.

This analysis shows that overheating the steam generator can be precluded for all utilizations by following the delineated control strategy. Cathode off-gas must be fed to the steam generator and the afterburner in the ratios specified by Figs. 6 and 7. Additionally, the steam generator must be operated above its maximum rated operating point of 400 °C, up to 550 °C, in exchange for a shorter service life. Finally, this analysis assumes a high efficiency steam generator. The operating region that meets all constraints is the intersection of the light-shaded regions of Figs. 6 and 7. (Ideally, with greater resources allocated to it, the steam generator could employ a more complex control strategy, in which flow rates are varied in real time as a function of the steam generator's temperature.)

4. Conclusion

Following both control strategies outlined previously, the afterburner sub-system should be operated in accordance with the recommended operating regions of Figs. 5–7. The intersection of recommended operating regions in these figures (highlighted in light shading) is the sub-system-wide recommended operating region, shown in Fig. 8. This sub-system-wide operating region incorporates both Solutions 1 and 2 to the two problems discussed earlier.

The control of the afterburner sub-system is crucial to the performance of the overall CHP FCS. This sub-system (1) determines the extent of thermal energy recovered from the system, up to 55% of fuel energy input; (2) establishes the rate limiting step in the control of the overall CHP FCS based on its response time; and (3) impacts upstream mass and energy flows strongly, such as the system's overall water balance, as this is the point in the system where the CHP FCS becomes closed loop for heat and mass flows. The control of the afterburner sub-system can be developed by detailed modeling design studies, such as the one presented. Detailed modeling studies, which can help define a system's overall control strategy, are crucial to the commercial success of CHP FCSs.

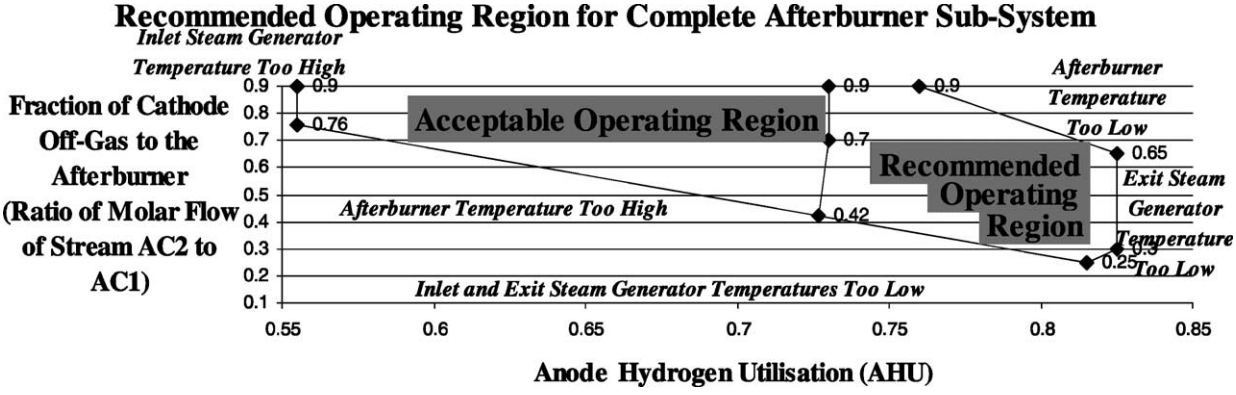

Fig. 8. Summarizes the recommended operating region for the complete afterburner sub-system. This region is highlighted in light shading and encompassed by a series of dark coordinates. It represents the combination of various constraints on the system in conjunction with an effective control system that meets these constraints.

References

[1] W.G. Colella, Design options for achieving a rapidly variable heat-to-power ratio in a combined heat and power (CHP) fuel cell system, J. Power Sources 106 (2002) 388–396.
[2] W.G. Colella, Combined heat and power fuel cell systems, Ph.D. Thesis, Department of Engineering Sciences, The University of Oxford, Oxford, 2002.
[3] C. Seymour, Commercial Acceptability of Solid Polymer Fuel Cell Systems in the Role of Combined Heat and Power Packages, Department of Trade and Industry (DTI), London, UK, 1998.
[4] Figure Adapted from Afterburner, Internal Report, Johnson Matthey Technology Centre (JMTC), Reading, UK, 2001.
[5] S.J. Cooper, D. Thompsett, A.C.C. Tseung, K.Y. Chen, Co-Tolerant Anode Electrocatalysts for Impure Hydrogen Oxidation in Solid Polymer Fuel Cells, Department of Trade and Industry (DTI), London, UK, 1997.
[6] G. Mepsted, Investigation of the Effects of Air Contaminants on SPFC Performance, Department of Trade and Industry (DTI), London, UK, 2001.
[7] J.M. Smith, H.C. Van Ness, Chemical Engineering Thermodynamics, third ed., McGraw-Hill, New York, 1975, p. 127.